Brain Pathology ISSN 1015-6305

RESEARCH ARTICLE

A New Targeted Model of Experimental Autoimmune Encephalomyelitis in the Common Marmoset

Ruth Martha Stassart[1]; Gunther Helms[2]; Enrique Garea-Rodríguez[3,4]; Stefan Nessler[1]; Liat Hayardeny[5]; Christiane Wegner[1]; Christina Schlumbohm[4,6]; Eberhard Fuchs[4,6,7]; Wolfgang Brück[1]

[1]Institute of Neuropathology, University Medical Center, Georg-August-University Göttingen, Göttingen, Germany, [2]Department of Cognitive Neurology, University Medical Center, Georg-August-University Göttingen, Göttingen, Germany, [3]Department of Neuroanatomy, Institute of Anatomy and Cell Biology, Albert-Ludwigs-University Freiburg, Freiburg, Germany, [4]Clinical Neurobiology Laboratory, German Primate Center, Göttingen, Germany, [5]Teva Pharmaceutical Industries, Netanya, Israel, [6]Encepharm GmbH, Göttingen, Germany, [7]Department of Neurology, University Medical Center, Georg-August-University Göttingen, Göttingen, Germany.

Keywords
common marmoset, demyelination, experimental autoimmune encephalomyelitis, immunomodulation, laquinimod, multiple sclerosis.

Corresponding author:
Ruth Martha Stassart, MD, Institute of Neuropathology, University Medical Center, Georg-August-University Göttingen, Göttingen, Germany (E-mail: *ruth.stassart@med.uni-goettingen.de*)

Received 30 April 2015
Accepted 20 July 2015
Published Online Article Accepted 24 July 2015

doi:10.1111/bpa.12292

Abstract

Multiple sclerosis (MS) is the most common cause for sustained disability in young adults, yet treatment options remain very limited. Although numerous therapeutic approaches have been effective in rodent models of experimental autoimmune encephalomyelitis (EAE), only few proved to be beneficial in patients with MS. Hence, there is a strong need for more predictive animal models. Within the past decade, EAE in the common marmoset evolved as a potent, alternative model for MS, with immunological and pathological features resembling more closely the human disease. However, an often very rapid and severe disease course hampers its implementation for systematic testing of new treatment strategies. We here developed a new focal model of EAE in the common marmoset, induced by myelin oligodendrocyte glycoprotein (MOG) immunization and stereotactic injections of proinflammatory cytokines. At the injection site of cytokines, confluent inflammatory demyelinating lesions developed that strongly resembled human MS lesions. In a proof-of-principle treatment study with the immunomodulatory compound laquinimod, we demonstrate that targeted EAE in marmosets provides a promising and valid tool for preclinical experimental treatment trials in MS research.

INTRODUCTION

Multiple sclerosis (MS) is a chronic neurological disorder of the central nervous system (CNS) characterized by multifocal inflammatory demyelinating lesions of white and gray matter. Although immunosuppressive and immunomodulatory therapeutics can attenuate the disease course, effective treatments that halt the disease on long term are still lacking (2, 4). The development of new treatment strategies depends on experimental animal models for MS, of which experimental autoimmune encephalomyelitis (EAE) in rodents is most commonly used. However, there is a striking discrepancy between the success of experimental therapies in murine EAE compared with the effectiveness of these treatments in subsequent clinical studies in MS (11). Indeed, the vast majority of new therapeutics does not reach drug approval in clinical trials due to lack of efficacy or safety concerns, with major implications for the participating patients (12). The high attrition rate further implies a significant economic burden for the pharmaceutical industry and contributing institutions (13).

The poor predictive value of EAE in rodents is considered as the main reason for the failed translation of experimental treatments, as the immunological background, the genetic basis and the disease course substantially differ from the human disease (11, 12). EAE in the new world monkey common marmoset (*Callithrix jacchus*) evolved as a promising alternative model for the testing of new treatment options and has been proposed to be particularly suited as a step in between experimental studies in rodents and clinical trials in patients (6, 11, 19, 22). Marmosets display a close neuroanatomical and immunological proximity to humans and the outbred nature reflects the genetic heterogeneity present in patients with MS (11, 22). Though, classical EAE in marmosets shows a pronounced variation and oftentimes a severe disease course, which hampers its use for systematic testing of new compounds and challenges ethical considerations (21). Classical EAE in marmosets has initially been induced by whole human myelin in combination with complete Freund's adjuvants (CFA), leading to a very acute and severe disease course (10, 11). This is why further studies adapted this protocol and induced EAE either with recombinant human myelin oligodendrocyte glycoprotein (rhMOG) or MOG peptide and CFA, followed by several booster injections with MOG in IFA (10, 11). These animals also develop pronounced neurological symptoms, including paresis and paralysis, but demonstrate a more variable disease course compared with whole human myelin (10, 11). More recently, injections of MOG

peptide in IFA alone have been shown to be sufficient to induce EAE in the common marmoset and other primates (7, 9, 11). This substantially improved the EAE model in marmosets, as CFA harbors a number of disadvantages such as side effects (eg, granulomatous reaction at the injection side) or the development of neutralizing antibodies against novel biologicals, which hampered the evaluation of treatment studies (7, 9, 11). However, EAE induced by rhMOG/IFA is still characterized by a variation of disease course and severity, with severely affected animals suffering from complete paralysis (7, 9).

Therefore, we here aimed at the development of a targeted, focal EAE model that circumvents the constraints of classical EAE in the common marmoset. To this end, we induced fEAE by recombinant rat myelin oligodendrocyte glycoprotein (MOG) immunization and intracerebral stereotactic injections of proinflammatory cytokines. At the injection site of cytokines, reproducible demyelinating lesions of the gray and white matter evolved, with histopathological features similar to human MS lesions. We demonstrate that lesions can be easily tracked by magnetic resonance imaging (MRI) and performed a first proof-of-principle therapy with the immunomodulatory drug laquinimod.

MATERIALS AND METHODS

Animals

Four male and six female adult common marmoset monkeys (*C. jacchus*) from the animal colony of ENCEPHARM, Göttingen, Germany, were investigated in this study. All animal experiments were carried out in accordance with the European Council Directive of September 2010 (2010/63/EU) and Communities Council Directive 86/609/EEC and were approved by the Lower Saxony Federal State Office for Consumer Protection and Food Safety (LAVES), Germany.

Induction of focal EAE and animal treatment

Animals were sedated with 0.15 mL of 10% ketamine and the injection sites were shaved and disinfected. Per animal either 12.5, 25 or 50 µg recombinant rat MOG emulsified in 600 µL of a mixture of incomplete Freund's adjuvant (IFA-DIFCO; Cat. No. 263910) and water (1:1) was subcutaneously injected at four sites: two near the shoulder and two near the loin region (see Figure 1B). Stereotactic injections were performed 70 days after immunization under general anesthesia with diazepam (0.3 mg/kg, i.m.), alphaxalon (10 mg/kg, i.m.) and glycopyrronium bromide (0.01 mg/animal, i.m.). General anesthesia was extended by inhalation anesthesia with 70:30 N_2O/O_2 in combination with isoflurane (0.5%–1.5%). The head of the anesthetized animal was fixed in a stereotaxic frame. The body was kept warm by a temperature-regulated electric cushion (37°C). After removal of the hair, a 2.5-cm medial incision was made and the periost around the bregma was removed. Under stereomicroscopic control, a small hole was drilled into the skull, 3 mm frontal and 3 mm lateral from the bregma at the coordinates AP 9.0 mm ML 3.5 mm with a sterile microdrill. The dura mater was punched with a Hamilton injection needle of the sterile automatic syringe while it was carefully pushed forward into a position of 3 mm depth from the outer surface of the dura mater. Next, 2 µg tumor necrosis factor-α (TNF-α) and 1.2 µg interferon-γ (IFN-γ) solved in 4 µL of phosphate buffered saline (PBS) was injected into the left hemisphere. A trace of Monastral blue (0.1%–0.2% final concentration) was added for better visualization of the injection track when preparing sections for histology. Intracerebral injections were made with a rate of 0.5 µL/min. Skin was sutured with resorptive material. Animals received an antibiotic treatment for 5 days after surgery (enrofloxacin; Baytril® 5%, Bayer AG, Leverkusen, Germany, 0.2 mL/day and animal) and pain treatment (meloxicam) for 3 days after surgery. Control animals were non-treated. For the proof-of-principle treatment trial, three marmosets received a prophylactic dose of 4 mg/kg/day laquinimod orally from the day of immunization on until the end of the study. Body weight was registered daily. Animals were scored in regular intervals and were equipped with miniActiwatches® to quantify potential impairments due to focal EAE lesions.

Enzyme-linked immunosorbent assay

Blood samples were centrifuged to separate the serum, in which the titer of MOG-specific antibodies was determined by enzyme-linked immunosorbent assay (ELISA) as described earlier (16). Briefly, recombinant purified MOG (rMOG) corresponding to the N-terminal sequence of rat MOG was coated on a 96-well Maxi Sorp plate (Nunc, Wiesbaden, Germany) at a concentration of 8 mg/mL. Sera were pre-diluted 40-fold and then titrated in three-fold dilutions throughout 12 steps in 5% (w/v) bovine serum albumin (BSA) in PBS. Detection was carried out with immunoglobulin G (IgG)-specific horseradish peroxidase-conjugated goat anti-rat antibodies (1:5000; Pierce, Rockford, IL, USA) with 3,3′,5,5′-tetramethylbenzidine (BM-Blue, POD; Roche, Basel, Switzerland) added as a substrate. Optical density was measured at 450 nm. Antibody titers were defined as the serum dilutions yielding absorption of twofold background levels. The number of animals analyzed in this experiment was as follows: 12.5 µg MOG: n = 2 for each time point; 25 µg MOG 21 days n = 2, 28 days n = 4, 78 days n = 2, 94 days n = 2; 50 µg MOG 21 days n = 2, 28 days n = 3, 78 days n = 1; 94 days n = 1. At least two technical replicates were performed for each animal.

MRI

MRI was performed under general anesthesia as described earlier. Animals were scanned in a 3T MRI system (Magnetom TIM Trio, Siemens Healthcare, Erlangen, Germany) using a human wrist coil (In Vivo, Gainesville, FA, USA) for signal reception. Marmosets were placed in supine position with head and upper spine inside the coil with the three-dimensional (3D) imaging volumes in transversal orientation. As anatomical reference, T1-weighted MRI was performed with an MP-RAGE sequence at 0.4 mm resolution (120 slices, 4:18 min). For detection of white matter lesions, T2-weighted MRI was performed at 0.33 mm resolution using a TSE sequence with variable flip angles (144 slices, 14:58 min, 5 averages). To detect acute inflammation, T1-weighted MRI was repeated after intravenous application of gadolinium-based contrast agent (Gadovist, Bayer-Schering, Berlin, Germany, 0.3 mmol/kg body weight). No uptake of gadolinium contrast agent in fEAE lesions was observed. Further details are described in Ref. (8).

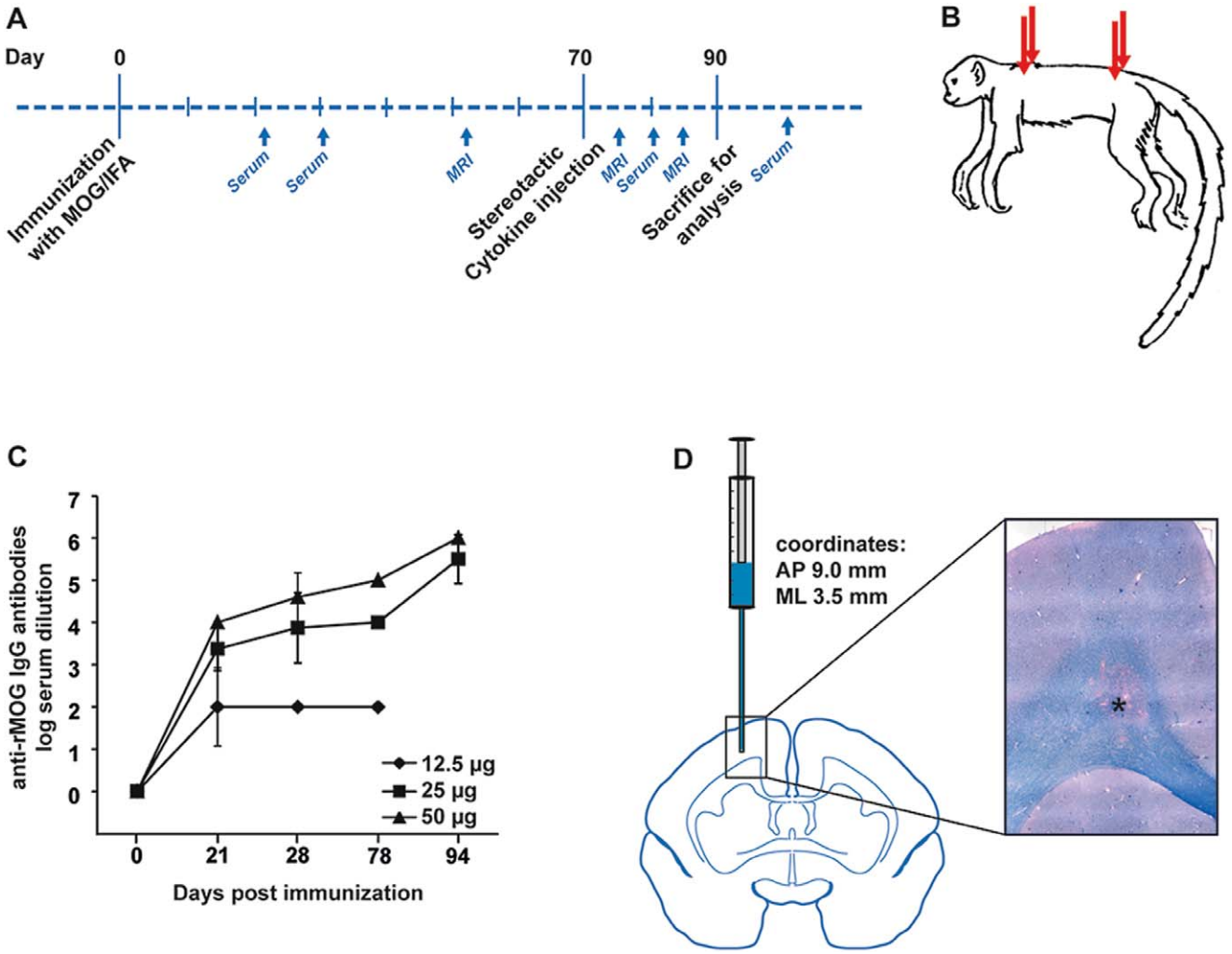

Figure 1. A. Schematic overview demonstrating the experimental strategy for the induction of focal experimental autoimmune encephalomyelitis (EAE) in the common marmoset. B. Immunization with subclinical dosages of recombinant myelin oligodendrocyte glycoprotein (rMOG) was performed subcutaneously at four injection sites. C. Marmosets were immunized subclinically with different dosages of rMOG (12.5, 25 and 50 µg) and serum concentrations of anti-MOG immunoglobulin G (IgG) antibodies were determined at 21, 28, 78 and 94 days post immunization by enzyme-linked immunosorbent assay (ELISA). The applied rMOG concentrations correlated with the IgG titers, which reached similar levels in animals immunized with 25 or 50 µg, respectively. Mean, SD; IgG antibodies shown as log of serum dilution. N, numbers are given within the Materials and Methods section. D. Proinflammatory cytokines were injected intracerebrally with the help of a stereotactic instrument at the coordinates AP (anteroposterior) 9.0 mm and ML (mediolateral) 3.5 mm, resulting in lesions of the corpus callosum and adjacent grey matter, as indicated on the schematic marmoset brain cross section. The light microscopic image represents a demyelinating lesion in the corpus callosum (see asterisk) as visualized by Luxol fast blue–periodic acid Schiff (LFB-PAS) staining, which marks myelin in blue.

Histology and immunohistochemistry

At study end, animals were anesthetized with diazepam (0.3 mg/kg, i.m., 0.025 mL) and alphaxalon (10 mg/kg, i.m., max. 0.5 mL) followed by a lethal dose of ketamine. Immediately after heart arrest, the animals were transcardially perfused with a fixative containing 4% 0.1 M sodium phosphate buffered paraformaldehyde (pH 7.4). Heads were post-fixed in buffered paraformaldehyde; after 24 h, the brains were carefully removed from the skull, dissected and embedded in paraffin. Histologic evaluation was performed on 3-µm-thick sections. Histological staining comprised hematoxylin–eosin (HE), Luxol fast blue–periodic acid Schiff (LFB-PAS) and Bielschowsky silver impregnation. For immunohistochemistry, the following primary antibodies were used: rabbit anti-myelin basic protein (MBP, 1:500, DAKO, Hamburg, Germany), rat anti-CD3 (1:50, mAb CD3-12, AbD Serotec, Puchheim, Germany), mouse anti-CD20 (1:50, mAb L26, DAKO, Hamburg, Germany) and mouse anti-myeloid-related protein 14 (MRP14, clone MAC387, 1:100, GeneTex, Irvine, CA, USA), rabbit anti-NOGO-A(H-300) (1:1000, Fa. St. Cruz

SC-25660), rabbit anti OLIG2 (1:1000 Fa. IBL Lot. 1B-327), rabbit anti-glial fibrillary acidic protein (anti-GFAP) (1:1000 Fa. DAKO), mouse anti-Alzheimer precursor protein (APP) (1:2000, Fa. Millipore, clone 22C11). Bound antibody was visualized using an avidin-biotin technique (ABC) with 3,3′-diaminobenzidine as chromogen. Control sections were incubated in the absence of primary antibody, with isotype control antibodies or with non-immune sera. Slides were counterstained using Mayer's hemalum solution.

Data analysis and statistics

Digital images of stained sections were obtained by light microscopy and a digital camera [Color View II, Olympus, Hamburg, Germany with the software CellA (Soft Imaging System, Olympus Soft Imaging Solutions, Münster, Germany)]. Images were processed by using NIH (National Institutes of Health, Bethesda, Maryland, USA) ImageJ, Photoshop CS (Adobe) and Illustrator 10 (Adobe) software. Statistical analysis was performed using the software Statistica 10.0 (StatSoft, Tulsa, OK, USA). Statistical differences over all groups were determined using either the Student's *t*-test or the chi-square test. Statistical differences were considered to be significant when $P < 0.05$ ($*P < 0.05$, $**P < 0.01$, $***P < 0.001$).

RESULTS

Targeted injection of cytokines after immunization leads to focal demyelination

In a first dose-finding experiment, adult marmosets were immunized subclinically with different dosages of recombinant rat MOG (rMOG) in IFA (Figure 1A,B). We applied MOG dosages of 12.5, 25 or 50 μg and analyzed the serum levels of IgG antibodies against rMOG at different time points after immunization (Figure 1C). IgG titers were detectable in all groups 21 days after immunization, and reached levels of classical EAE in marmosets when animals were immunized with 25 or 50 μg rMOG, respectively (Figure 1C and data not shown). As 25 and 50 μg rMOG induced comparable IgG serum concentrations (Figure 1C), all further experiments were performed with a dosage of 25 μg MOG emulsified in IFA.

In order to induce focal demyelinating lesions, we next performed stereotactic cytokine injections intracerebrally when anti-MOG titers reached a first plateau phase in marmosets (after 70 days) (Figure 1C,D). In detail, the proinflammatory cytokines IFN-γ (1.2 μg) and TNF-α (2 μg) were injected into the left hemisphere targeting the cortex and corpus callosum (Figure 1D), thereby adapting a protocol previously established in rats (16). Importantly, all but one animal (6 out of 7) developed reproducible demyelinating lesions of gray and white matter within a predictable time frame of 3 weeks after lesion induction by cytokine injection (Figure 1D, Table 1). Of note, marmosets showed no changes in body weight or general behavior after lesion induction (Supporting Information Figure S1A).

In vivo MRI constitutes a sensitive tool for lesion detection

We then asked whether lesion development can be followed by MRI imaging after intracerebral cytokine injections. All animals received control T1- and T2-weighted cerebral MRI scan after immunization but before intracerebral injections as baseline record and to rule out brain affection in response to MOG immunization (Figure 2). Importantly, we previously demonstrated that control intracerebral injections in marmosets did not lead to MRI detectable brain damage (8). Indeed, previous studies in rodent and marmoset EAE models support the specificity of MRI imaging for the detection of demyelinating lesions in the CNS (1, 18).

Ensuing MRI was performed 1 week after cytokine application, where lesion formation could already be visualized, with lesions localizing to the site of stereotactic injections (Figure 2). Lesions could be likewise identified 2 weeks after cytokine injection (Figure 2). The lesion size was comparable to the first time point in T1- and T2-weighted images (Figure 2).

Table 1. Summary of the analyzed animals showing the respective experimental group, gender, age at experiment onset as well as the lesion size, which was quantified on light microscopic images.

Clinical animal ID	Group	Sex	Age at experiment onset (months)	Lesion area (mm^2)
1	Ctrl	F	52	3.92
2	Ctrl	F	24	1.12
3	Ctrl	M	26	5.36
4	Ctrl	F	42	1.11
5	Ctrl	F	26	0.21
6	Ctrl	F	51	0.03
7	Ctrl	M	53	—
8	Laq	M	29	—
9	Laq	F	42	—
10	Laq	M	42	—

Confluent demyelinating lesions evolved at the injection site of cytokines

The histopathological evaluation revealed demyelinating lesions of gray and white matter at the site of stereotactic cytokine injections. While the majority of lesions (4 out of 6) evolved to be large and confluent demyelinating lesions (Figure 3A, Table 1) reminiscent of human MS plaques (20), two lesions appeared mainly perivascular and smaller in size, similar to those observed in brain biopsies of patients with ADEM (acute disseminated encephalomyelitis) (20) (Table 1, Supporting Information Figure S1B). Large and confluent lesions were characterized by complete demyelination with a highly increased cellularity (Figure 3A,B). The lesion edge appeared well demarcated from the adjacent periplaque white matter (Figure 3C,D). Although distended, axons remained relatively preserved within the lesion area (Figure 3E,F).

Histopathology in focal EAE resembles human MS lesions

Do the demyelinating lesions of focal EAE in marmosets reflect the histopathological features of human MS plaques?

Human MS lesions can be classified according to the demyelinating activity in either active or inactive lesions (14). Early active MS lesions are characterized by ongoing myelin disintegration,

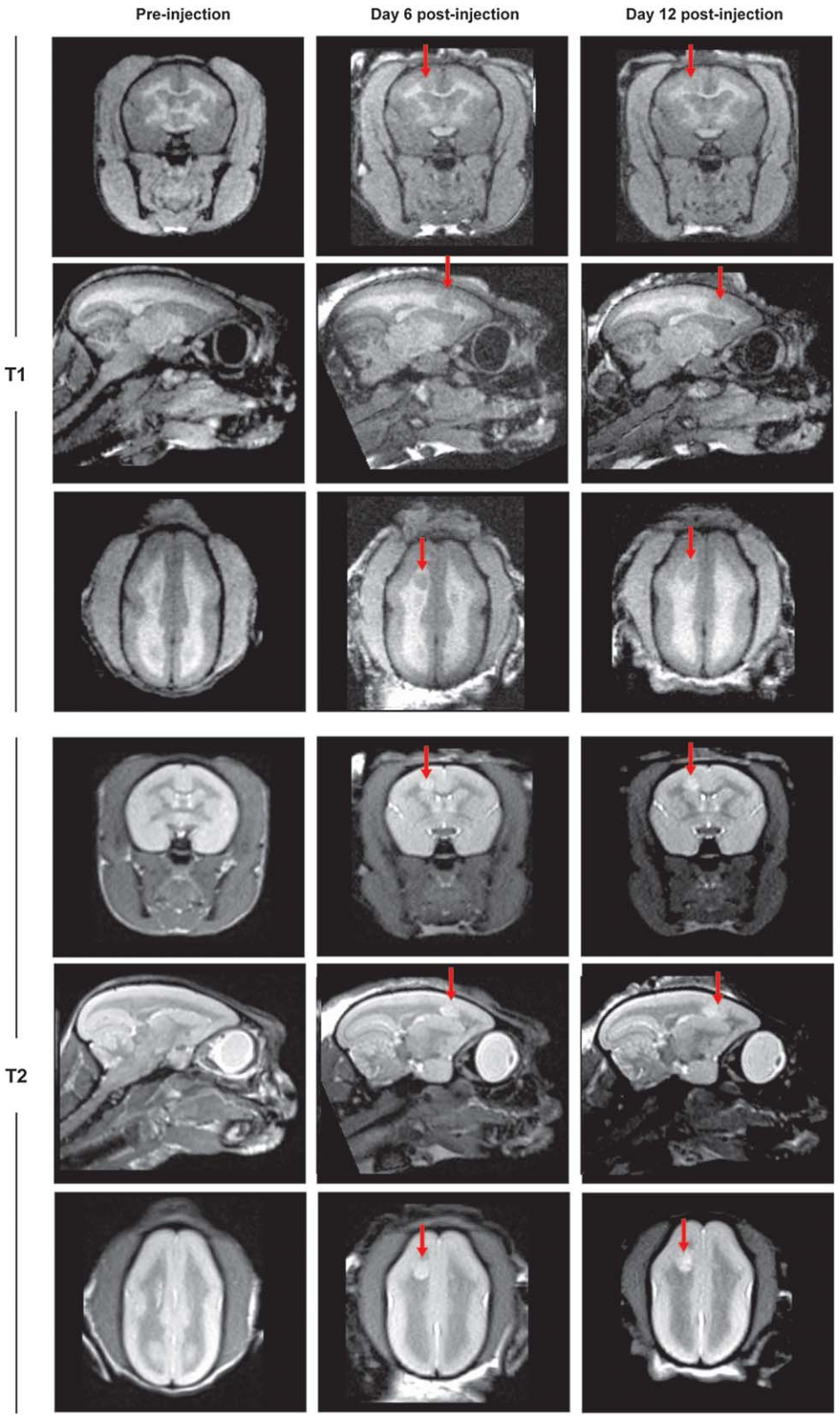

Figure 2. Representative T1- and T2-weighted magnetic resonance imaging (MRI) images of a marmoset brain in coronal, sagittal and transverse planes. Images were performed at three different time points to allow the analysis of lesion development. The first imaging was performed after immunization but before cytokine injection (Pre-injection), followed by MRI at day 6 and 12 post lesion induction by cytokine injections. Lesions are indicated by arrows.

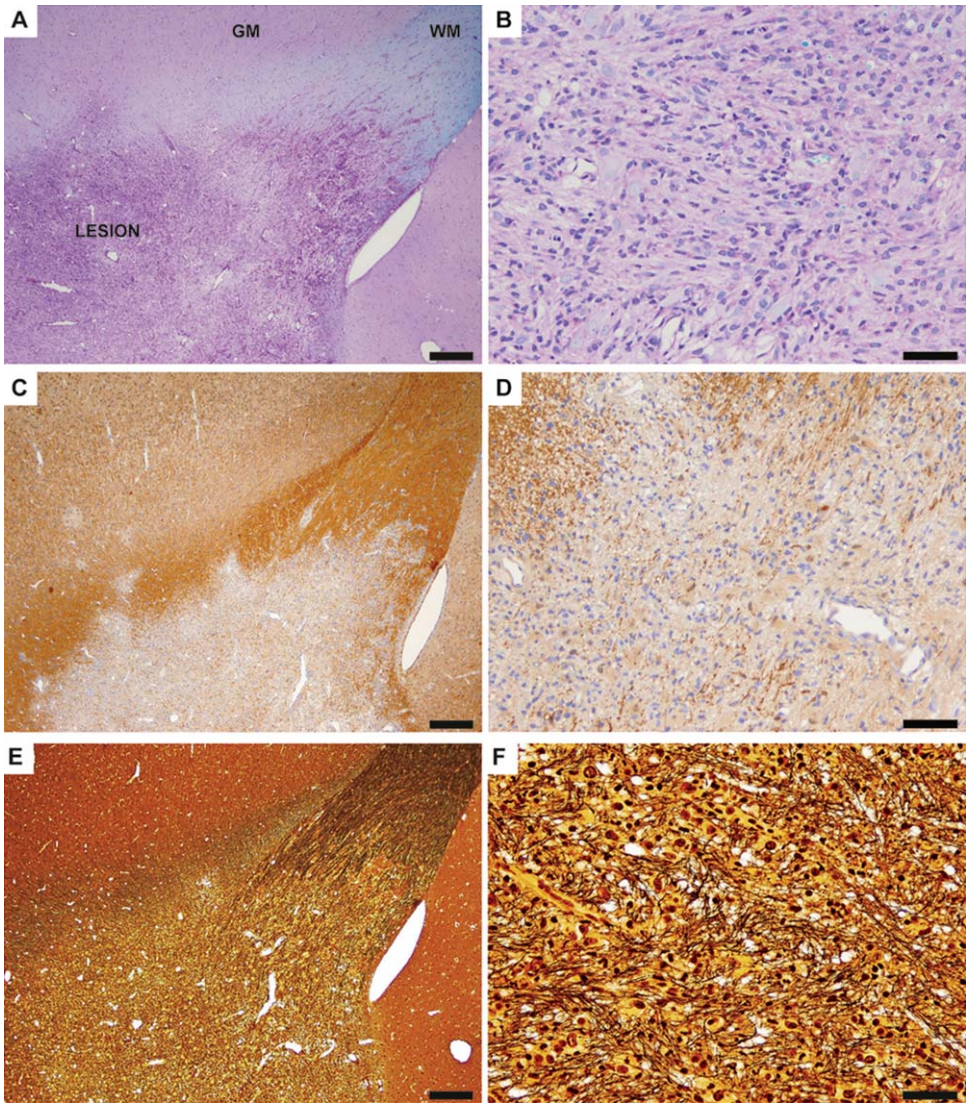

Figure 3. Representative light microscopic images depict a demyelinating lesion of the corpus callosum and neighboring gray matter of focal experimental autoimmune encephalomyelitis (fEAE) in marmosets (20 days post lesion induction by the injection of cytokines). A. A low magnification overview demonstrates the demyelinated area (LESION) and the transition to the normal appearing white matter (WM) and gray matter (GM). Luxol fast blue–periodic acid Schiff (LFB-PAS) staining, scale bar 200 μm. B. In a higher magnification, complete demyelination and a strongly increased cellularity becomes apparent. LFB-PAS staining, scale bar 50 μm. C. Overview of a lesion stained with an antibody against myelin basic protein (MBP) demonstrates a sharp border between the demyelinated area and the adjacent white and gray matter. Scale bar 200 μm. D. MBP immunohistochemistry confirms complete demyelination within the lesion area at a higher magnification. Scale bar: 50 μm. E. A Bielschowsky silver impregnation was performed to visualize axonal density within the lesion. Scale bar 200 μm. F. Note that axons are distended but remain relatively preserved in the lesion. Bielschowsky silver impregnation. Scale bar 50 μm.

which is histologically reflected by the infiltration of macrophages that incorporate myelin degradation products (12). In detail, macrophages in active MS lesions express the myeloid-related protein-14 (MRP14), indicating recent activation (3). In addition, macrophages show cytoplasmic inclusions of minor myelin proteins such as CNP (2′,3′-cyclic-nucleotide-3′-phosphodiesterase) and MOG (myelin oligodendrocyte glycoprotein), which cannot be detected in older MS lesions anymore (14). In order to compare demyelinating lesions of focal EAE in the common marmoset to human MS lesions, we hence first tested whether lesions in marmosets are undergoing active demyelination. To this end, we performed immunohistochemistry against MRP14, which indeed revealed a pronounced infiltration of MRP14-positive macrophages, similar to early active human MS lesions (Figure 4A,B). In line, we detected myelin degradation products of CNP and MOG in macrophages of both, marmoset and human MS lesions (Figure 4 C,D and data not shown).

Hence, lesions of fEAE in the common marmoset demonstrate, 3 weeks after lesion induction, the distinctive features of early active demyelinating lesions, which prompted us to further inves-

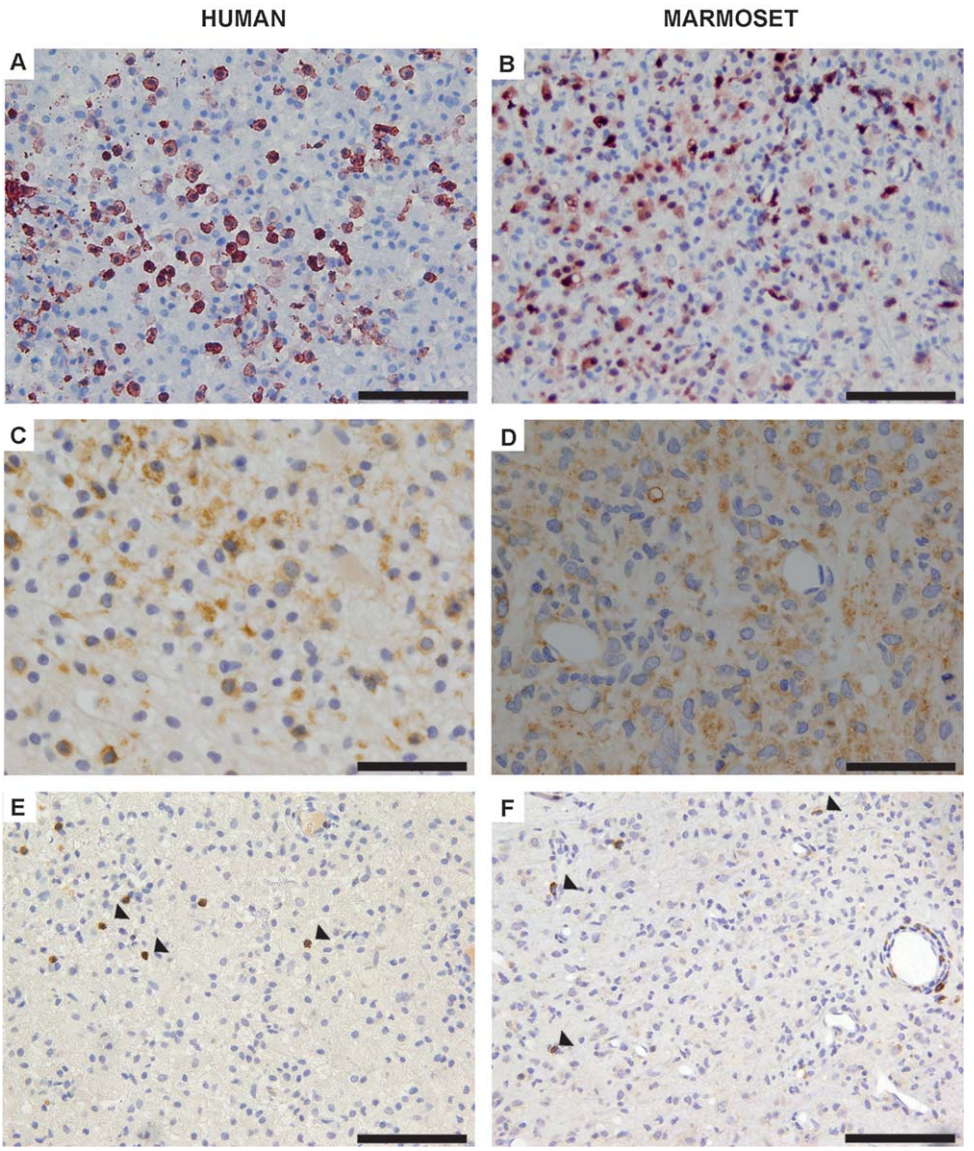

Figure 4. A. Representative image of an early active human multiple sclerosis (MS) plaque, which reveals a prominent infiltration of early active macrophages as determined by myeloid-related protein 14 (MRP14) immunohistochemistry. Scale bar 100 μm. B. The infiltration of numerous MRP14-positive macrophages also characterizes demyelinating lesions of focal experimental autoimmune encephalomyelitis (fEAE) in marmosets. Scale bar 100 μm. C. Macrophages in human MS lesions demonstrate intracytoplasmic myelin oligodendrocyte glycoprotein (MOG)-positive degradation products as revealed by immunohistochemistry. Scale bar 100 μm. D. MOG-positive myelin degradation products are also detected within macrophages of demyelinating lesions in the common marmoset. Scale bar 100 μm. E. T-cells (arrowheads) are homogeneously distributed within lesions of human MS. CD3 immunohistochemistry; scale bar 100 μm. F. Likewise, a comparable, diffuse T-cell infiltration (arrowheads) with a perivascular accentuation is detected in fEAE lesions. CD3 immunohistochemistry, scale bar 100 μm.

tigate the histopathological characteristics in comparison to early active human MS lesions of three different patients.

We first analyzed the total number of cells within lesions, which revealed an interindividual variation in cell densities in both, MS and fEAE lesions, but no significant differences between the two groups, although cell numbers were slightly higher in marmosets (Supporting Information Figure S1C). Like human MS lesions, demyelinating areas in fEAE displayed a diffuse distribution of T-cells (Figure 4E,F) and a prominent reactive astrocytosis, as determined by GFAP immunohistochemistry (Figure 5A,B,G). Oligodendrocytes were present in all demyelinating lesions of fEAE, with comparable numbers of mature NOGO-A positive glial cells in human and marmoset lesions (Figure 5C,D,H). As previously described for human MS (12), we furthermore detected numerous OLIG2-positive cells in fEAE that outnumbered NOGO-A positive oligodendrocytes, reflecting the presence of

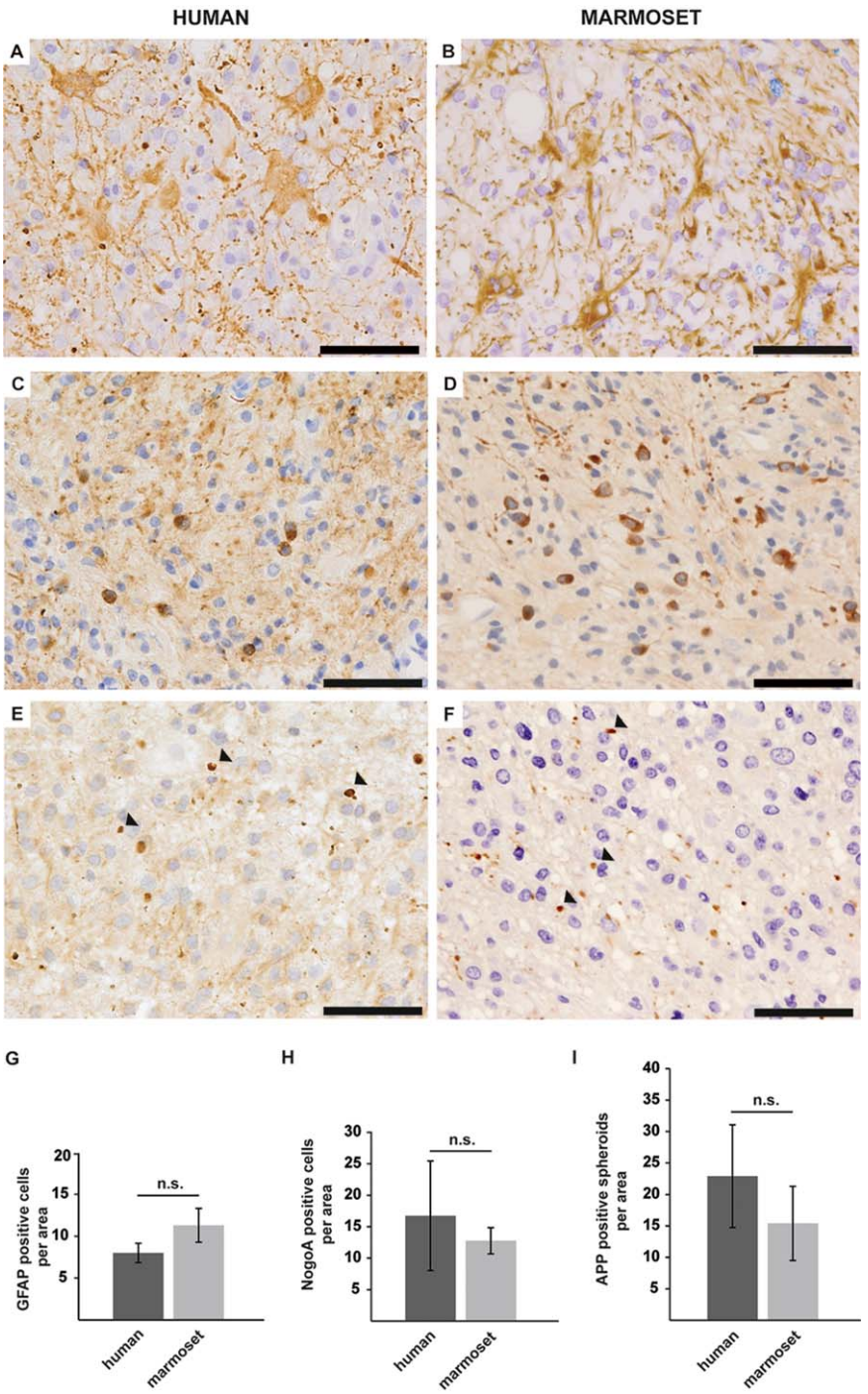

Figure 5. A. Glial fibrillary acidic protein (GFAP) immunohistochemistry reveals a reactive astrocytosis in human multiple sclerosis (MS) lesions. Scale bar 50 μm. B. A prominent astrogliosis is as well a feature of focal experimental autoimmune encephalomyelitis (fEAE) lesions in marmosets. GFAP immunohistochemistry. Scale bar 50 μm. C. Numerous NOGO-A positive oligodendrocytes are detected within demyelinated areas of human MS plaques. Scale bar 50 μm. D. Likewise, NOGO-A positive oligodendrocytes are abundantly detected in lesions of fEAE in marmosets. Scale bar 50 μm. E. Anti-Alzheimer precursor protein (APP) immunohistochemistry reveals axonal damage in MS lesions, as exemplarily indicated by arrowheads. Scale bar 50 μm. F. Axonal degeneration is likewise observed in fEAE lesion (see arrowheads). APP immunohistochemistry. Scale bar 50 μm. G. The quantification of GFAP-positive cells per area (0.04 mm^2) reveals a similar degree of astrogliosis in human (n = 3) and marmoset (n = 4) lesions. Mean, SD, n.s. = non-significant. H. The number of NOGO-A-positive oligodendrocytes in human MS lesions (n = 3) varies between individual patients, but is overall comparable to the density of oligodendrocytes in marmoset fEAE (n = 4). Quantification per area (0.04 mm^2), mean, SD, n.s. = non-significant. I. APP-positive axonal spheroids are detectable in both, human (n = 3) and marmoset (n = 3) lesions to a similar extent. However, the interindividual variability is much higher in human MS lesions. Quantification per area (0.04 mm^2), mean, SD, n.s. = nonsignificant.

oligodendrocyte precursor cells within demyelinated areas (Supporting Information Figure S1D). In addition to the cellular composition of demyelinating lesions, we analyzed axonal impairment by APP immunohistochemistry (Figure 5E,F,I). The extent of axonal damage substantially varied between individual cases, but again was overall comparable between marmoset and human lesions (Figure 5E,F,I). We conclude that the histopathology of active demyelinating lesions in fEAE in marmosets closely resembles early active human MS and may therefore constitute a valuable tool for preclinical therapeutic trials.

A prophylactic therapy with laquinimod prevents lesion formation in fEAE

In a next step, we investigated the applicability of the established fEAE model in a proof-of-principle experimental therapy trial. Can a modulation of the immune system in a prophylactic treatment approach influence lesion formation in fEAE? We treated marmosets with a new immunomodulator, laquinimod, in a dosage of 4 mg/kg per day from the time point of immunization until the sacrifice of the animals 20 days after cytokine injections. Laquinimod is active when applied orally and has been recently tested in two phase III clinical trials (2). Strikingly, while six out of seven control animals showed demyelinating lesions at study end, none of the laquinimod-treated marmosets (n = 3) developed demyelinating lesions, as determined by LFB-PAS staining and MBP immunohistochemistry ($P = 0.01$, chi-square test) (Figure 6). Only a minor astrocytic and microglial reaction was observed at the stereotactic injection site of laquinimod-treated animals (Supporting Information Figure S2). Importantly, also sequential MRI analyses revealed no lesion formation in laquinimod-treated animals (Figure 7). Thus, modulating the immune system before lesion induction by intracerebral cytokine injections can completely prevent the development of fEAE in marmosets.

DISCUSSION

The translation of new research findings from experimental studies in animals to human patients with MS is substantially hampered by the lack of adequate disease models (8). In the present study, we therefore aimed at the development of a new animal model for MS. Within the past decade, the common marmoset has emerged as a promising alternative model organism, as it closely resembles the human immune system and better reflects the genetic diversity of patients when compared to rodent models (8, 22). The development of classical EAE in marmosets thus represented an important step toward more predictable animal models for MS, although it does not fully meet the requirements necessary for an implementation in routine preclinical trials. In particular, the clinical impairment in classical EAE leads to increased dropout rates, and a high disease burden raises ethical concern in non-human primates. Furthermore, the variability in the time course of disease development and the heterogeneity of lesion localization complicates the interpretation of study results.

Here, we have developed a model of focal autoimmune encephalomyelitis in the common marmoset by subclinical immunization with rMOG and intracerebral injections of proinflammatory cytokines. All but one marmoset (86% of the animals) developed demyelinating lesions within a predictable time frame after lesion induction. We demonstrate that lesion formation is detected at an early stage and can be reliably followed by MRI, which thus constitutes a valid tool for monitoring of treatment trials in this model. Lesion evolved at the injection site of cytokines, which facilitated their localization in histological sections, and enabled the comparison of lesion characteristics in identical anatomical regions. Notably, we detected two different types of demyelinating lesions in marmosets. The majority of animals depicted large confluent demyelinating lesions, similar to typical lesions in human MS (20). However, some marmosets displayed small, perivascular foci of demyelination, as observed in ADEM (20).

The presence of these two different lesion types opens the possibility to compare the histopathological characteristics of ADEM and MS-like lesions and to evaluate differential therapeutic effects in these lesions. Though, the detection of minor treatment benefits may be hampered if both lesion types are evaluated together. In this case, it appears reasonable to concentrate the analyses on the more prevalent group of large demyelinating lesions.

Demyelinating lesions in our model predominantly localized to the white matter of the corpus callosum, but also comprised the adjacent gray matter. Indeed, cortical lesions have previously been shown to arise after cytokine injections in pre-immunized rats (5, 15). However, do lesions of fEAE reflect the histopathological features of human MS plaques? In order to answer this question, we first analyzed the immune cell infiltration in marmoset lesions. Importantly, we detected a pronounced infiltration of macrophages expressing MRP14 in all lesions. The acute stage inflammatory macrophage marker MRP14 has been identified to be specifically expressed in active lesions of human MS biopsies (3). We hence selected early active demyelinating lesions of MS biopsies for a further comparison to fEAE lesions in marmosets. A detailed analysis of marmoset and human lesions revealed, next to a similar pattern of inflammation, comparable cell densities within areas of complete demyelination, along with equivalent numbers of reactive astrocytes and oligodendrocytes. Likewise, while axons remained largely well preserved, axonal damage was observed in both, MS and fEAE lesions to a similar degree.

Early active MS lesions show a profound heterogeneity with regard to the pathology of demyelination, which can be classified into four different patterns of myelin disintegration (14). Among those, pattern II is characterized by antibody and complement depositions within demyelinating lesions (14). A pattern II-like histopathology has been previously identified in models of classical, MOG induced EAE in the common marmoset in both, cortical and white matter lesions (15, 17). In addition, complement depositions were detected in the rat model of focal, targeted EAE (16). However, C9 depositions in this rat model were most pronounced in the first days after cytokine injection during ongoing cortical inflammation and demyelination, which suggests that complement deposition is only transiently detectable during early disease stages (16). In line with these findings, we did not detect robust complement and antibody deposits in demyelinating lesions of targeted EAE in the common marmoset, as we examined the lesions at a later time point, which is 3 weeks after lesion induction. This time point was chosen for optimal correlation with the MRI analyses.

In conclusion, we here provide, to the best of our knowledge, the first direct histological comparison between demyelinating lesions

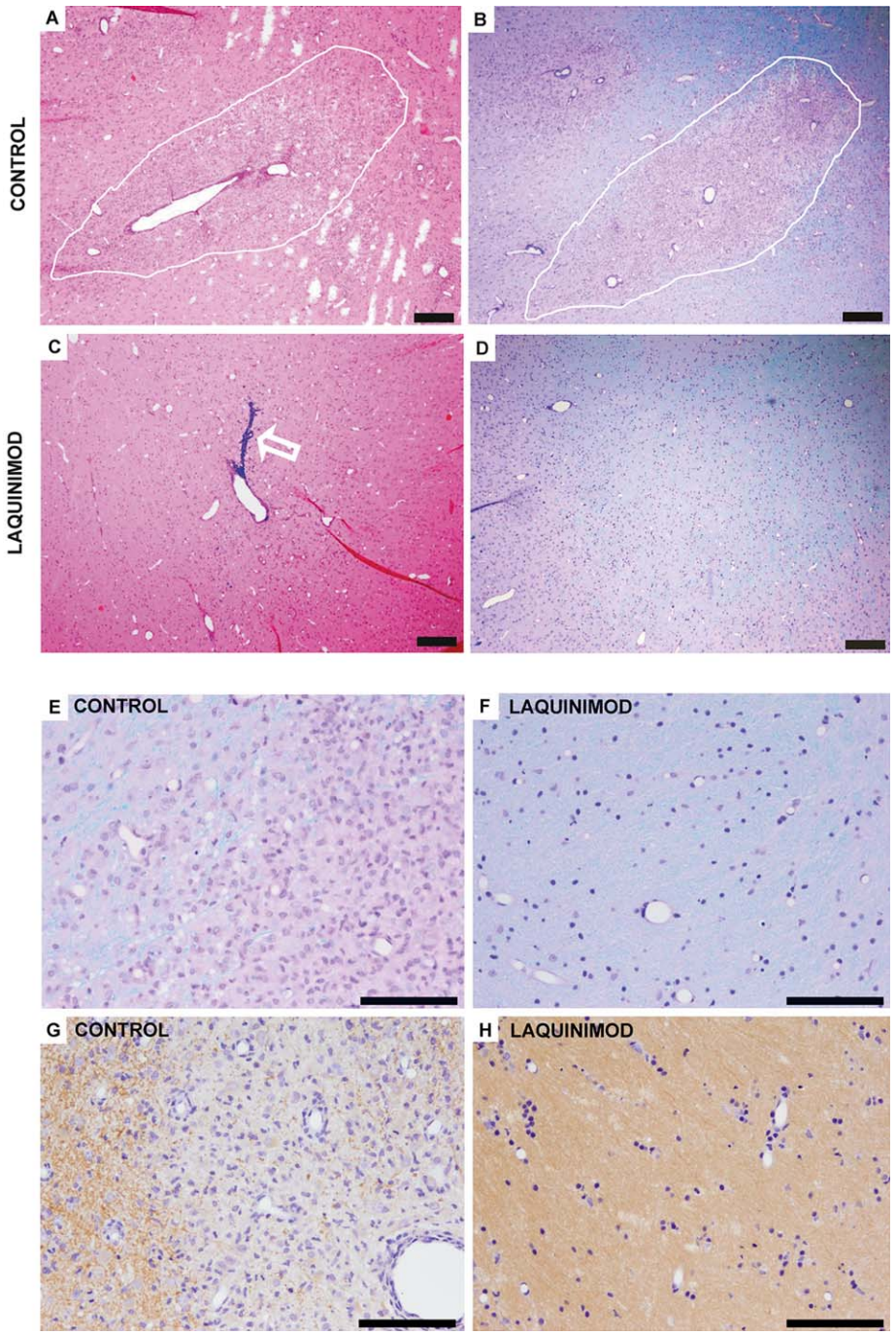

Figure 6. A. Representative light microscopic overview of a demyelinating lesion (indicated by white line) in a marmoset with focal experimental autoimmune encephalomyelitis (fEAE). Hematoxylin–eosin (HE) staining, scale bar 200 μm. B. Luxol fast blue–periodic acid Schiff (LFB-PAS) staining of the same animal as (A) reveals complete demyelination within the lesion. Scale bar 200 μm. C. Representative image of the injection site of cytokines in a marmoset which received a prophylactic treatment of the immunomodulatory drug laquinimod. Note the injection channel, which is marked by Monastral blue (see arrow). Scale bar 200 μm. D. In the respective LFB-PAS staining of the marmoset described in (C), no lesion formation can be detected. Scale bar 200 μm. E. The lesion edge of a control animal is demonstrated at a higher magnification of the LFB-PAS staining (see B). The lesion shows complete demyelination and an increased cell number. Scale bar 100 μm. F. In contrast, no signs of demyelination can be detected in laquinimod treated marmosets. Representative image of the injection site of cytokines in a higher magnification. LFB-PAS staining, scale bar 50 μm. G. myelin basic protein (MBP) immunohistochemistry of a control animal demonstrates MBP-positive myelin sheaths at the lesion edge (left part of the image) whereas the lesion itself shows complete demyelination (see right part of the image). Scale bar 100 μm. H. In laquinimod-treated animals no loss of MBP-positive myelin sheaths can be detected. Representative image of the injection site of cytokines in a higher magnification. MBP immunohistochemistry, scale bar 100 μm.

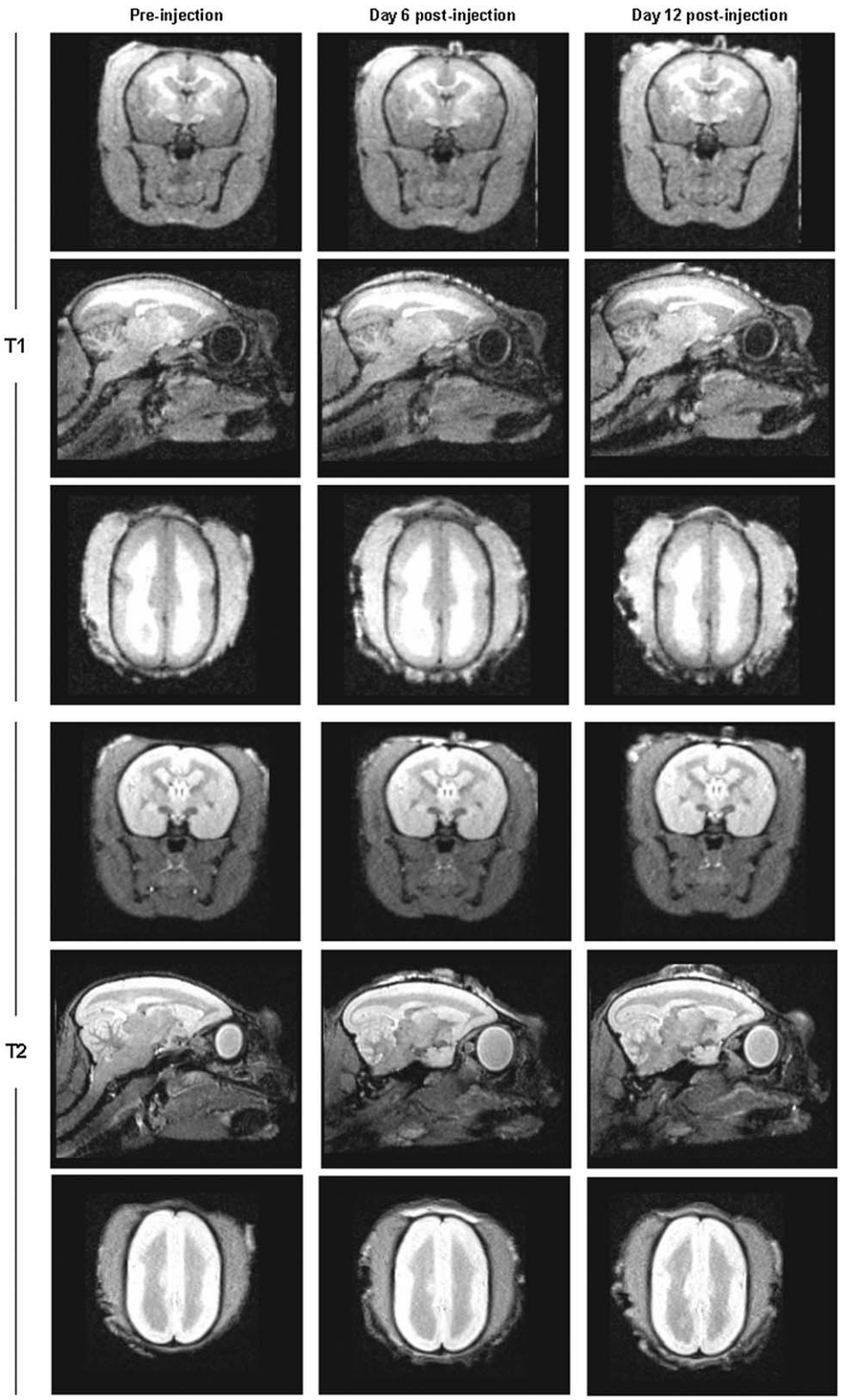

Figure 7. Representative T1- and T2-weighted magnetic resonance imaging (MRI) images of the brain of a marmoset that received a prophylactic laquinimod treatment. Shown are the coronal, sagittal and transverse planes. Images were performed at three different time points to allow the analysis of lesion development. The first imaging was performed after immunization but before cytokine injection (Pre-injection), followed by MRI at day 6 and 12 post lesion induction by cytokine injections. Importantly, MRI imaging revealed no lesion formation in marmosets that were treated with laquinimod.

in marmosets and humans. We demonstrate that demyelinating lesions of humans and marmosets share the major histopathological hallmarks, which renders fEAE in marmosets a valid model for active stages of MS. Importantly, induction of fEAE in marmosets showed no side effects and all analyzed animals remained healthy until the study end.

These results finally prompted us to investigate the applicability of the newly established fEAE in a first therapeutic study. Indeed, a prophylactic treatment (ie. before immunization of the animals) with the immunomodulator laquinimod was able to completely prevent lesion formation in marmosets. Laquinimod is a new, orally active immunomodulatory drug, which has been recently tested in clinical phase III trials (2). Interestingly, laquinimod has been shown to not only exert effects on the peripheral immune response but also to additionally harbor a CNS-intrinsic mode of action (2). How laquinimod prevents lesion development in fEAE, and whether it exerts direct effects on the production of anti-MOG antibodies in fEAE, though, has to be evaluated in future studies.

In conclusion, we established a new focal model of EAE in the common marmoset and demonstrate that demyelinating lesions in fEAE closely resemble to early active human MS plaques. We propose targeted EAE as a valid and promising tool for future preclinical studies in MS research.

CONFLICT OF INTEREST

The authors have nothing to disclose and no conflict of interest to report.

ACKNOWLEDGMENTS

We thank Astrid Wohltmann for expert technical assistance and Sandra Leineweber as well as Olaf Rautz for expert animal care.

REFERENCES

1. Boretius S, Schmelting B, Watanabe T, Merkler D, Tammer R, Czéh B *et al* (2006) Monitoring of EAE onset and progression in the common marmoset monkey by sequential high-resolution 3D MRI. *NMR Biomed* **19**:41–49.
2. Brück W, Vollmer T (2013) Multiple sclerosis: oral laquinimod for MS—bringing the brain into focus. *Nat Rev Neurol* **9**:664–665.
3. Brück W, Porada P, Poser S, Rieckmann P, Hanefeld F, Kretzschmar HA, Lassmann H (1995) Monocyte/macrophage differentiation in early multiple sclerosis lesions. *Ann Neurol* **38**:788–796.
4. Brück W, Gold R, Lund BT, Oreja-Guevara C, Prat A, Spencer CM *et al* (2013) Therapeutic decisions in multiple sclerosis: moving beyond efficacy. *JAMA Neurol* **70**:1315–1324.
5. Gardner C, Magliozzi R, Durrenberger PF, Howell OW, Rundle J, Reynolds R (2013) Cortical grey matter demyelination can be induced by elevated pro-inflammatory cytokines in the subarachnoid space of MOG-immunized rats. *Brain* **136**:3596–3608.
6. Genain CP, Hauser SL (2001) Experimental allergic encephalomyelitis in the New World monkey *Callithrix jacchus*. *Immunol Rev* **183**:159–172.
7. Haanstra KG, Jagessar SA, Bauchet A-L, Dousseau M, Fovet C-M, Heijmans N *et al* (2013) Induction of experimental autoimmune encephalomyelitis with recombinant human myelin oligodendrocyte glycoprotein in incomplete Freund's adjuvant in three non-human species. *J Neuroimmune Pharmacol* **5**:1251–1264.
8. Helms G, Garea-Rodriguez E, Schlumbohm C, König J, Dechent P, Fuchs E *et al* (2013) Structural and quantitative neuroimaging of the common marmoset monkey using a clinical MRI system. *J Neurosci Methods* **215**:121–131.
9. Jagessar SA, Kap YS, Heijmans N, van Driel N, van Straalen L, Bajramovic JJ *et al* (2010) Induction of progressive demyelinating autoimmune encephalomyelitis in common marmoset monkeys using MOG34-56 peptide in incomplete Freund adjuvant. *J Neuropathol Exp Neurol* **69**:372–385.
10. Jagessar SA, Vierboom M, Blezer EL, Bauer J, Hart BA, Kap YS (2013) Overview of models, methods, and reagents developed for translational autoimmunity research in the common marmoset (*Callithrix jacchus*). *Exp Anim* **62**:159–171.
11. Kap YS, Laman JD, 't Hart BA (2010) Experimental autoimmune encephalomyelitis in the common marmoset, a bridge between rodent EAE and multiple sclerosis for immunotherapy development. *J Neuroimmune Pharmacol* **5**:220–230.
12. Kola I, Landis J (2004) Can the pharmaceutical industry reduce attrition rates? *Nat Rev Drug Discov* **3**:711–715.
13. Kuhlmann T, Miron V, Cui Q, Wegner C, Antel J, Brück W (2008) Differentiation block of oligodendroglial progenitor cells as a cause for remyelination failure in chronic multiple sclerosis. *Brain* **131**:1749–1758.
14. Lassmann H, Brück W, Lucchinetti C (2001) Heterogeneity of multiple sclerosis pathogenesis: implications for diagnosis and therapy. *Trends Mol Med* **3**:115–121.
15. Merkler D, Böschke R, Schmelting B, Czéh B, Fuchs E, Brück W *et al* (2006) Differential macrophage/microglia activation in neocortical EAE lesions in the marmoset monkey. *Brain Pathol* **16**:117–123.
16. Merkler D, Ernsting T, Kerschensteiner M, Brück W, Stadelmann C (2006) A new focal EAE model of cortical demyelination: multiple sclerosis-like lesions with rapid resolution of inflammation and extensive remyelination. *Brain* **129**:1972–1983.
17. Merkler D, Schmelting B, Czéh B, Fuchs E, Stadelmann C, Brück W (2006) Myelin oligodendrocyte glycoprotein-induced experimental autoimmune encephalomyelitis in the common marmoset reflects the immunopathology of pattern II multiple sclerosis lesions. *Mult Scler* **12**:369–374.
18. Nessler S, Boretius S, Stadelmann C, Bitter A, Merkler D, Hartung HP *et al* (2007) Early MRI changes in a mouse model of multiple sclerosis are predictive of severe inflammatory tissue damage. *Brain* **130**:2186–2198.
19. Pomeroy IM, Matthews PM, Frank JA, Jordan EK, Esiri MM (2005) Demyelinated neocortical lesions in marmoset autoimmune encephalomyelitis mimic those in multiple sclerosis. *Brain* **128**:2713–2721.
20. Popescu BF, Lucchinetti CF (2012) Pathology of demyelinating diseases. *Annu Rev Pathol* **7**:185–217.
21. 't Hart BA, Massacesi L (2009) Clinical, pathological, and immunologic aspects of the multiple sclerosis model in common marmosets (*Callithrix jacchus*). *J Neuropathol Exp Neurol* **68**:341–355.
22. 't Hart BA, Laman JD, Bauer J, Blezer E, van Kooyk Y, Hintzen RQ (2004) Modelling of multiple sclerosis: lessons learned in a non-human primate. *Lancet Neurol* **3**:588–597.

SUPPORTING INFORMATION

Additional Supporting Information may be found in the online version of this article at the publisher's web-site:

Figure S1. A. Marmosets showed no changes in body weight when comparing the day of immunization (day 0) with the end of

experiment (day 90). N = 3 per time point, mean, SD, n.s. = non significant. **B.** Light-microscopic overview demonstrating small, perivascular accentuated lesions (indicated by arrowheads), which were observed in a subset of marmosets with fEAE. LFB-PAS staining, Scale bar 200 μm. **C.** The total number of cells per area (0.04 mm^2) was quantified on light microscopic images and revealed comparable cell densities within demyelinating lesions of human and marmoset. N = 3 per group. Mean, SD, n.s. = non significant. **D.** Numerous OLIG2 positive cells were detected within demyelinating lesions of fEAE in marmosets. Scale bar 50 μm.

Figure S2. A, B. Laquinimod treated animals demonstrate reactive astrocytes at the injection side of cytokines as determined by GFAP immunohistochemistry (**A** overview, scale bar 200 μm; **B** higher magnification, scale bar 100 μm). **C, D.** MRP14 immunohistochemistry reveals a minor microglial reaction to the injection of cytokines in laquinimod treated animals. (**C** overview, scale bar 200 μm; **D** higher magnification, scale bar 100 μm).